Ultrasonics 52 (2012) 215–222

Contents lists available at SciVerse ScienceDirect

Ultrasonics

journal homepage: www.elsevier.com/locate/ultras

Using ultrasound Nakagami imaging to assess liver fibrosis in rats

Ming-Chih Ho [a], Jen-Jen Lin [b], Yu-Chen Shu [c], Chiung-Nien Chen [a], King-Jen Chang [a,d], Chien-Cheng Chang [e,f,*], Po-Hsiang Tsui [g,*]

[a] Department of Surgery, National Taiwan University Hospital and College of Medicine, National Taiwan University, Taipei, Taiwan, ROC
[b] Department of Applied Statistics and Information Science, Ming Chuan University, Taoyuan, Taiwan, ROC
[c] Department of Mathematics, National Cheng Kung University, Tainan, Taiwan, ROC
[d] Department of Surgery, Cheng Ching General Hospital, Taichung, Taiwan, ROC
[e] Institute of Applied Mechanics, National Taiwan University, Taipei, Taiwan, ROC
[f] Research Center for Applied Sciences, Academia Sinica, Taipei, Taiwan, ROC
[g] Department of Medical Imaging and Radiological Sciences, College of Medicine, Chang Gung University, Taoyuan, Taiwan, ROC

ARTICLE INFO

Article history:
Received 16 June 2011
Received in revised form 11 August 2011
Accepted 12 August 2011
Available online 22 August 2011

Keywords:
Rat liver fibrosis
Nakagami distribution
Backscattering

ABSTRACT

This study explored the feasibility of using the ultrasound Nakagami image to assess the degree of liver fibrosis in rats. The rat has been widely used as a model in investigations of liver fibrosis. Ultrasound grayscale imaging makes it possible to observe fibrotic rat livers in real time. Statistical analysis of the envelopes of signals backscattered from rat livers may provide useful clues about the degree of liver fibrosis. The Nakagami-model-based image has been shown to be useful for characterizing scatterers in tissues by reflecting the echo statistics, and hence the Nakagami image may serve as a functional imaging tool for quantifying rat liver fibrosis. To validate this idea, fibrosis was induced in each rat liver ($n = 21$) by an intraperitoneal injection of 0.5% dimethylnitrosamine. Livers were excised from rats for *in vitro* ultrasound scanning using a single-element transducer. The backscattered-signal envelopes of the acquired raw ultrasound signals were used for Nakagami imaging. The Metavir score determined by a pathologist was used to histologically quantify the degree of liver fibrosis. It was found that the Nakagami image could be used to distinguish different degrees of liver fibrosis in rats, since the average Nakagami parameter increased from 0.55 to 0.83 as the fibrosis score increased from 0 (i.e., normal) to 4. This correlation may be due to liver fibrosis in rats involving an increase in the concentration of local scatterers and the appearance of the periodic structures or clustering of scatterers that would change the backscattering statistics. The current findings indicate that the ultrasound Nakagami image has great potential as a functional imaging tool to complement the use of the conventional B-scan in animal studies of liver fibrosis.

1. Introduction

Chronic infection with viral hepatitis is a critical cause of liver cirrhosis and its sequelae [1]. Identifying the degree of liver fibrosis is important for estimating the prognosis, surveillance, and treatment decisions in patients with chronic viral hepatitis. A liver histological diagnosis based on the use of a needle biopsy is the gold standard for liver fibrosis assessments, but this cannot be performed routinely in the clinic because it is an invasive method associated with patient discomfort and, in rare cases, with serious complications. The accuracy of the liver biopsy method can also adversely affected by sampling errors [2,3]. Thus, many researchers have focused on developing noninvasive imaging technologies as a routine tool for the assessment of liver fibrosis.

Before performing clinical trials involving humans, feasibility studies must be performed on animal models. The rat is a very popular animal model for studying liver fibrosis [4–7]. In order to conveniently observe the formation of liver fibrosis without sacrificing rats, researchers need imaging tools that provide real-time examination capabilities. Ultrasound grayscale (i.e., B-mode) imaging is a very convenient and powerful tool for animal research due to its low cost, use of nonionizing radiation, noninvasiveness, and portability. Nevertheless, the conventional B-mode image only qualitatively describes tissue structures and is unsuitable for quantitative analyses of scatterer properties [8–10].

Developing new techniques to complement the B-scan may make it possible to characterize scatterers in tissues. Liver tissue may be considered to comprise a three-dimensional arrangement

* Corresponding authors. Addresses: Institute of Applied Mechanics, National Taiwan university, Taipei, Taiwan, ROC (C.C. Chang), Department of Medical Imaging and Radiological Sciences, College of Medicine, Chang Gung University, 259 Wen-Hwa 1st Road, Kwei-Shan, Tao-Yuan 333, Taiwan, ROC. Tel.: +886 3 2118800x3795; fax: +886 3 2118700 (P.-H. Tsui).

E-mail addresses: mechang@iam.ntu.edu.tw (C.-C. Chang), tsuiph@mail.cgu.edu.tw(P.-H. Tsui).

0041-624X/$ - see front matter © 2011 Elsevier B.V. All rights reserved.
doi:10.1016/j.ultras.2011.08.005

of many scatterers. Excitation by an ultrasound transducer will result in the production of echoes from these scatterers. This ultrasound backscattering is essentially a random process, and therefore the statistical analysis of the ultrasound signals backscattered from livers may further provide some useful clues about the scatterer properties of livers for use in fibrosis assessments.

The Nakagami statistical distribution has received considerable attention in the field of medical ultrasound, because the associated Nakagami parameter can be used to identify various probability density functions (pdfs) of the backscattered signals, making it possible to characterize scatterers in a tissue [11–15]. The need for imaging tools that can visually identify scatterer properties in clinical and research applications further prompted the development of the ultrasound Nakagami image. The concept of Nakagami imaging originated from the suggestion of Shankar [16] and some other preliminary studies [17,18]. The method for constructing the Nakagami image was established in these and subsequent pilot studies [19,20]. It has been shown that Nakagami imaging is capable of visualizing the difference in scatterer concentration between normal and abnormal tissues, complementing the conventional B-mode image and thereby improving diagnoses [21–26].

The present study aimed to determine the feasibility of using Nakagami imaging to assess liver fibrosis in rats. Like the B-scan, the Nakagami image is based on a standard pulse-echo system configuration, but the difference is that the Nakagami image may provide scatterer information about rat liver fibrosis that complements that in the B-scan. This idea was tested by obtaining B-mode and Nakagami images of rat livers having different degrees of fibrosis formation *in vitro*. The usefulness of the Nakagami image in identifying the degree of rat liver fibrosis was evaluated.

This paper is organized as follows: Section 2 introduces the theoretical background, Section 3 describes the experimental materials and methods, Section 4 presents the results, and Section 5 discusses the experimental findings and draws conclusions.

2. Theoretical background

The Nakagami parameter is a shape parameter of the Nakagami statistical distribution, as given by [11]

$$f(r) = \frac{2m^m r^{2m-1}}{\Gamma(m)\Omega^m} \exp\left(-\frac{m}{\Omega} r^2\right) U(r), \tag{1}$$

where $\Gamma(\cdot)$ and $U(\cdot)$ are the gamma function and the unit step function, respectively. Let $E(\cdot)$ denote the statistical mean; then scaling parameter Ω and Nakagami parameter m associated with the Nakagami distribution can be respectively obtained from

$$\Omega = E(R^2) \tag{2}$$

and

$$m = \frac{[E(R^2)]^2}{E[R^2 - E(R^2)]^2}. \tag{3}$$

Variation of the Nakagami parameter from 0 to 1 means a change in the envelope statistics from a pre-Rayleigh to a Rayleigh distribution, and a Nakagami parameter larger than 1 means that the backscattering statistics conform to a post-Rayleigh distribution.

According to previous studies [11,12,19], the pdf of the backscattered-signal envelope would follow the Rayleigh distribution when the resolution cell of the ultrasound transducer contains a large number of randomly distributed scatterers. If the resolution cell contains scatterers that have randomly varying scattering cross sections with a comparatively high degree of variation, the envelope statistics conform to pre-Rayleigh distributions. If the resolution cell contains periodically located scatterers in addition to randomly distributed scatterers, the envelope statistics follow post-Rayleigh distributions. It has been shown that the Nakagami distribution with a pdf shape determined by the Nakagami parameter is highly consistent with the envelope histogram of the ultrasound backscattered signals [11], and hence the Nakagami distribution provides a general model for ultrasound backscattering.

The process of Nakagami imaging is detailed elsewhere [19]. In brief, the Nakagami image is based on the Nakagami parameter map, which is constructed by using a local sliding window to process the raw envelope image. This involves first using a window within the envelope image to collect the local backscattered-signal envelopes for estimating the local Nakagami parameter (m_w), which is assigned as the new pixel located in the center of the window. This step is then repeated with the window moving throughout the entire envelope image in steps of one pixel, which yields the Nakagami image as the map of m_w values. The window size determines the resolution of the Nakagami image: using a smaller window will improve the resolution but it will also yield fewer envelope data points, which can lead to unstable estimates of m_w (overestimation). Therefore, prior to constructing the Nakagami image it is necessary to determine the optimal size of the window that can simultaneously satisfy the stable estimation of m_w and an acceptable resolution of the Nakagami image.

In this study the window size was determined according to our previously proposed procedure [19]. First, a reference homogeneous medium was scanned to obtain its envelope image. Each envelope signal of the image scan line was used to calculate Nakagami parameter m. The average Nakagami parameter, $\bar{m}$, was calculated by averaging all m values, which represented the global backscattering statistics of the scanned region. Second, each m_w value in the scanned region and average value $\bar{m}_w$ were subsequently estimated using progressively larger sliding windows. When the window was large enough to ensure the stable estimation of m_w, $\bar{m}_w$ would approach $\bar{m}$ to reflect the identical backscattering statistics. Consequently, the optimal window size was determined once $\bar{m}_w = \bar{m}$.

Based on the conclusion in our previous study [19], using a window with a side length corresponding to three times the pulse length of the incident ultrasound to construct the Nakagami image can simultaneously satisfy both stable estimations of m_w and an acceptable imaging resolution. The above criterion was established based on measurements made using a 5 MHz transducer [19]. Subsequent studies have demonstrated that same criterion for determining the window size is also suitable when using different ultrasound transducers, including high-frequency transducers (35–60 MHz) [21,22] and commercial array transducers (7 MHz) [23,24]. For this reason, the side length of the window used to construct the Nakagami image in the present study was three times the pulse length of the employed transducer.

3. Materials and methods

3.1. Animal experiments

Twenty-one 7-week-old male Wistar rats weighing between 210 and 230 g were used. The institutional animal care and use committee at Taiwan University Hospital approved the use of the rats in this study. The rats were bred and maintained in an air-conditioned animal house with food and water. Liver fibrosis was induced in each rat by an intraperitoneal injection of 0.5% dimethylnitrosamine (DMN) at 2 ml/kg body weight for three consecutive days each week [27]. In order to induce different degrees of liver fibrosis in the rats, DMN was injected for different numbers of weeks, as illustrated in Fig. 1. Each group comprised three rats. Group 1 was the normal case, and animals in groups 2, 3, 4,

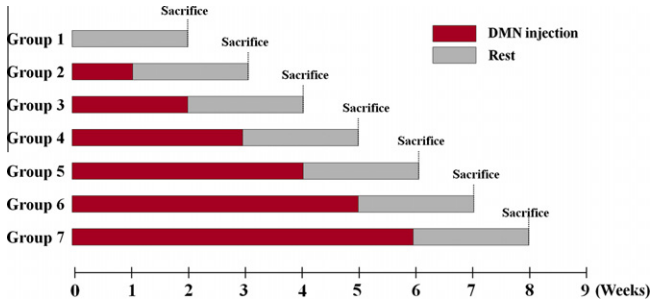

Fig. 1. Schedule of DMN injections in each group.

5, 6, and 7 received DMN injections for 1, 2, 3, 4, 5, and 6 weeks, respectively. Each rat was sacrificed after a rest period of 2 weeks, and the liver was excised. Ultrasound scanning was applied to the left lateral lobe of the liver. The left lobe had a thickness of 1.0–1.5 cm, and a length and width of 2–4 cm.

3.2. Data acquisition

A single-crystal ultrasound imaging system was constructed for scanning the liver *in vitro* to acquire the ultrasound backscattered signals associated with different degrees of liver fibrosis. The system comprised a mechanical scanning assembly, a single-element transducer, a pulser/receiver, and a data acquisition card, as shown in Fig. 2 and explained below. The transducer was mechanically scanned using a high-resolution motion stage driven by a piezoelectric motor (Model HR8, Nanomotion, Yokneam, Israel); using a piezoelectric motor reduced the noise level and thereby improved the quality of the received ultrasound echoes. The transducer was driven by a pulser/receiver (Model 5072PR, Panametrics-NDT, Waltham, MA, USA) for transmitting and receiving ultrasound signals. The received radio-frequency (RF) signals backscattered from the liver were amplified by the built-in 59 dB amplifier in the pulse/receiver and then digitized by an analog-to-digital card (Model PXI-5152, National Instruments, Austin, TX, USA) for data storage and offline analysis in a personal computer.

A focused transducer with an element diameter of 6 mm was used (Model V310, Panametrics-NDT). Pulse-echo testing of the transducer revealed that its central frequency and pulse length were 6.5 MHz and 0.3 mm, respectively. The focal length was designed to be 1.1 cm, and therefore the theoretical −6 dB beam width calculated using the *f*-number was about 0.4 mm. We placed the transducer and liver samples on a holder in a bath containing

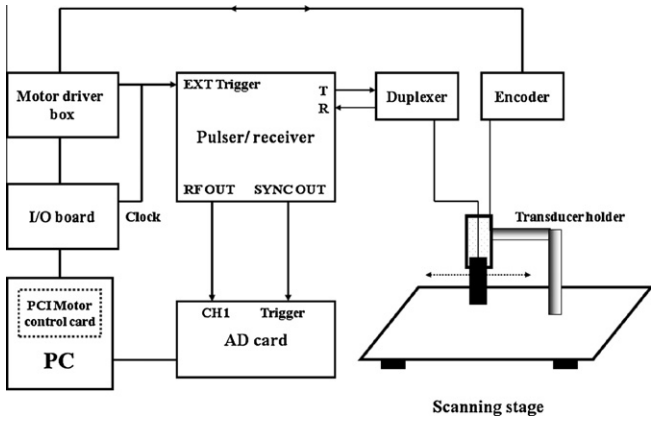

Fig. 2. System setup for ultrasound imaging measurements on liver specimens.

distilled water at room temperature. The liver was positioned at the focus of the transducer (i.e., 1.1 cm from it). We performed five independent B-scans of each liver specimen, each of which consisted of 100 A-lines of the backscattered signals obtained at a sampling rate of 50 MHz. Each backscattered signal corresponded to a data length of about 12 mm. The interval between each A-line was 0.1 mm. Each scan line was then demodulated using the Hilbert transform to obtain the envelope image, and the B-mode image was formed based on the logarithm-compressed envelope image at a dynamic range of 40 dB. The Nakagami image corresponding to each B-mode image was formed according to the algorithmic procedure described above. We constructed the Nakagami images using a square window with a size of $0.9 \times 0.9\ mm^2$.

The following pseudocolor scale was designed to maximize the display clarity of information in the Nakagami image: Nakagami parameters smaller than 1 were assigned blue shading that changed from dark to light as the value increased, representing backscattered-signal envelopes that conformed to various pre-Rayleigh statistical distributions; a value of 1 was shaded white to indicate a Rayleigh distribution; and values larger than 1 were assigned red shading from dark to light as the value increased, representing backscattered-signal envelopes that conformed to various post-Rayleigh statistical distributions.

3.3. Histological analysis

To score the level of liver fibrosis for each rat, the liver specimen was fixed in 10% neutral-buffered formalin, embedded in paraffin, and sliced into 4-μm-thick sections for histological analysis with the hematoxylin and eosin (H&E) staining method. The tissue sections used in the histological examinations were 10–15 mm in diameter, and the regions examined histologically did not necessarily correspond to the insonified regions. To avoid sampling errors, we prepared five histological sections from different areas of each liver specimen. The Metavir score, which quantifies the degree of liver fibrosis, was determined by an experienced pathologist who was blinded to the treatment protocol. The pathologist identified that homogeneously distributed fibrosis had been induced throughout the liver parenchyma, with the extent of liver fibrosis being proportional to the duration of DMN injections.

4. Results

Table 1 summarizes the Metavir scores of the rats as determined by the pathologist. A fibrosis score of '0' was assigned by the pathologist when the degree of liver fibrosis did not satisfy the scoring criterion for a fibrosis score of 1, and such cases were considered to be normal. Overall, the fibrosis score increased with the duration of DMN injections. There were 7, 5, 3, 3, and 3 rats with fibrosis scores of 0, 1, 2, 3, and 4, respectively. Fig. 3a shows typical H&E-stained sections for normal rat livers and for fibrotic rat livers with fibrosis scores of 1–4. The amount of the connective fibrous tissues extending out from the portal areas increased with the fibrosis score, demonstrating that DMN injections successfully induced liver fibrosis in the rats.

Fig. 3b shows B-mode images of rat livers with different degrees of fibrosis. It can be seen that the B-scan images did not reflect the progress of liver fibrosis in the rats, since the image intensity did not vary significantly with the fibrosis score—except for the image appearing to be brighter for a fibrosis score of 3, as demonstrated in Fig. 4a. Clinically, the echo intensity is the most convenient index for assessing fibrosis formation [28], since the formation of fibrotic structures increases the echogenicities of scatterers in the liver [29]. However, some previous studies have revealed that the echo intensity may not be a reliable index, possibly due to inade-

Table 1
Metavir scores of liver fibrosis in rats as determined by the pathologist.

Group number (n = 3 for each group)	Metavir scores of the three rats in each group
1	0, 0, 0
2	0, 0, 1
3	0, 1, 2
4	0, 1, 2
5	1, 4, 4
6	1, 3, 2
7	3, 4, 3

quate reproducibility in the grading and staging of liver fibrosis [28,30]. This problem also appeared to occur in our animal experiments.

The information provided by the Nakagami image about the degree of rat liver fibrosis differed from that available in the B-scan image. Fig. 3c shows that the shading of the Nakagami image appeared to be correlated with the formation of liver fibrosis in rats. The amount of the red–blue-interlaced[1] shading in Nakagami images of the rat livers increased with the fibrosis score. This feature of the Nakagami image was indicative of backscattering statistics in rat livers that partially followed pre-Rayleigh distributions and partially followed post-Rayleigh distributions. Moreover, the proportion of red shading in the Nakagami image appeared to increase with the degree of liver fibrosis. Blue shading predominated in the Nakagami image of a normal rat liver, while the amount of red shading (i.e., indicative of regions following post-Rayleigh distributions) increased with the fibrosis score. Fig. 4b shows the relationship between the average Nakagami parameter and the fibrosis score. The average Nakagami parameter was calculated from the pixel values in the Nakagami image corresponding to the liver region, which was manually tracked by a pathologist. The Nakagami parameter increased from 0.55 ± 0.07 (mean ± SD) to 0.83 ± 0.02, representing that the global statistics of the backscattered-signal envelope changed from a pre-Rayleigh distribution to a roughly Rayleigh distribution when the fibrosis score increased from 0 to 4. This result means that the average pixel value of the Nakagami image may be useful for scoring the degree of liver fibrosis in rats.

In order to further evaluate the usefulness of the Nakagami image in classifying normal and fibrotic livers, Fig. 5 compares the values of the Nakagami parameter between the normal group and the cases with different fibrosis scores. Fig. 5a and b compare the average Nakagami parameters between normal cases and those with fibrosis scores of 1 and 2, respectively. The probability values (i.e., p values) calculated using the independent-samples t-test were 0.54 and 0.07, respectively, meaning that the Nakagami image could not distinguish between normal livers and the early stage of liver fibrosis. Fig. 5c and d compare the average Nakagami parameters between normal cases and those with fibrosis scores of 3 and 4, respectively. These two comparisons produced p values smaller than 0.01, demonstrating that the Nakagami image could be used to distinguish between normal cases and the more-severe cases of fibrosis formation in rat livers.

Further comparisons were made to better understand the behavior and usefulness of the Nakagami image in assessments of rat liver fibrosis. We combined the rats into various group pairs, and compared the Nakagami parameters between them. Fig. 6a compares the Nakagami parameters of normal livers and fibrotic livers with scores of 1–4, for which the p value was 0.09. In contrast, the p value for the comparison between normal cases combined with those with a fibrosis score of 1 and those cases with scores of 2–4 was smaller than 0.01, as shown in Fig. 6b. The other two comparisons are shown in Fig. 6c and d, respectively. The results in Fig. 6 indicate that the Nakagami image can be used to distinguish between less-severe (scores < 2) and more-severe (scores of 2–4) cases of liver fibrosis in rats, while it cannot be used to distinguish between normal livers and cases with a fibrosis score of 1 (as also shown in Fig. 5).

[1] For interpretation of color in Fig. 3, the reader is referred to the web version of this article.

5. Discussion and conclusion

The experimental results obtained in this study have demonstrated that the Nakagami approach can be used to visualize and distinguish the degree of liver fibrosis in rats. It appears that the Nakagami parameter increased with the degree of liver fibrosis due to the increased proportion of the sample area in which the local backscattering statistics conformed to a post-Rayleigh distribution (i.e., red shading in the Nakagami image). The possible underlying reasons are discussed below.

Rat liver tissues contain blood vessels that typically backscatter ultrasound signals more strongly than do other liver tissues. A blood vessel in a rat liver acts like a strong point reflector, as shown in the B-scans in Fig. 3. Homogeneous liver tissue containing point reflectors would exhibit a relatively high variation in the backscattering cross-sections of scatterers, leading to a pre-Rayleigh distribution. In other words, the pre-Rayleigh distributions for normal rat liver tissue may be due to the effects of the blood vessels. On the other hand, the Nakagami image of the fibrotic liver contained more red regions, representing local post-Rayleigh distributions. It is well known that liver fibrosis is the result of the wound-healing response of the liver to repeated injury. After injury, parenchymal cells regenerate and replace the necrotic or apoptotic cells. Such a process is related to an inflammatory response and a limited deposition of extracellular matrix (ECM). A prolonged hepatic injury can result in the failure of liver regeneration, and with hepatocytes being substituted by abundant ECM [31]. The ECM is an interlocking mesh of fibrous proteins and glycosaminoglycans that provides structural support to cells, in addition to performing various other important functions. Thus, a greater severity of liver fibrosis may increase the concentration of local scatterers and the appearance of periodic structures or clustering of scatterers in the tissue background, resulting in the backscattered-signal envelopes conforming to a post-Rayleigh statistical distribution.

Our experimental results demonstrated that the Nakagami image is useful for visualizing the degree of rat liver fibrosis. However, this does not necessarily mean that the Nakagami image can be used to detect liver fibrosis in humans. Referring to the previous literature [32,33], we found that the results obtained in our animal study did not agree well with those from human researches. For example, Yamada et al. [32] excised human liver specimens from autopsies and placed them in a tank for ultrasound scanning by a commercial clinical ultrasound scanner operating at transmitting and receiving frequencies of 2 and 4 MHz, respectively, and found that the signals backscattered from normal liver tissues approximately conformed to a Rayleigh distribution, while those from liver tissues with cirrhosis conformed to a pre-Rayleigh distribution. We attribute this discrepancy to differences in the fiber characteristics between rats and humans.

Moreover, artifact problems may appear in the Nakagami image. The shadings in the top and bottom parts of each Nakagami image corresponded to the background signals in the B-mode image. The background signals mainly contain random white noise and the damping signal, which is the small unwanted residual vibration of the transducer excitation pulse. These signals could produce undesirable shadings (i.e., artifact) around the examined tissue. In the experiments, the same system, set-

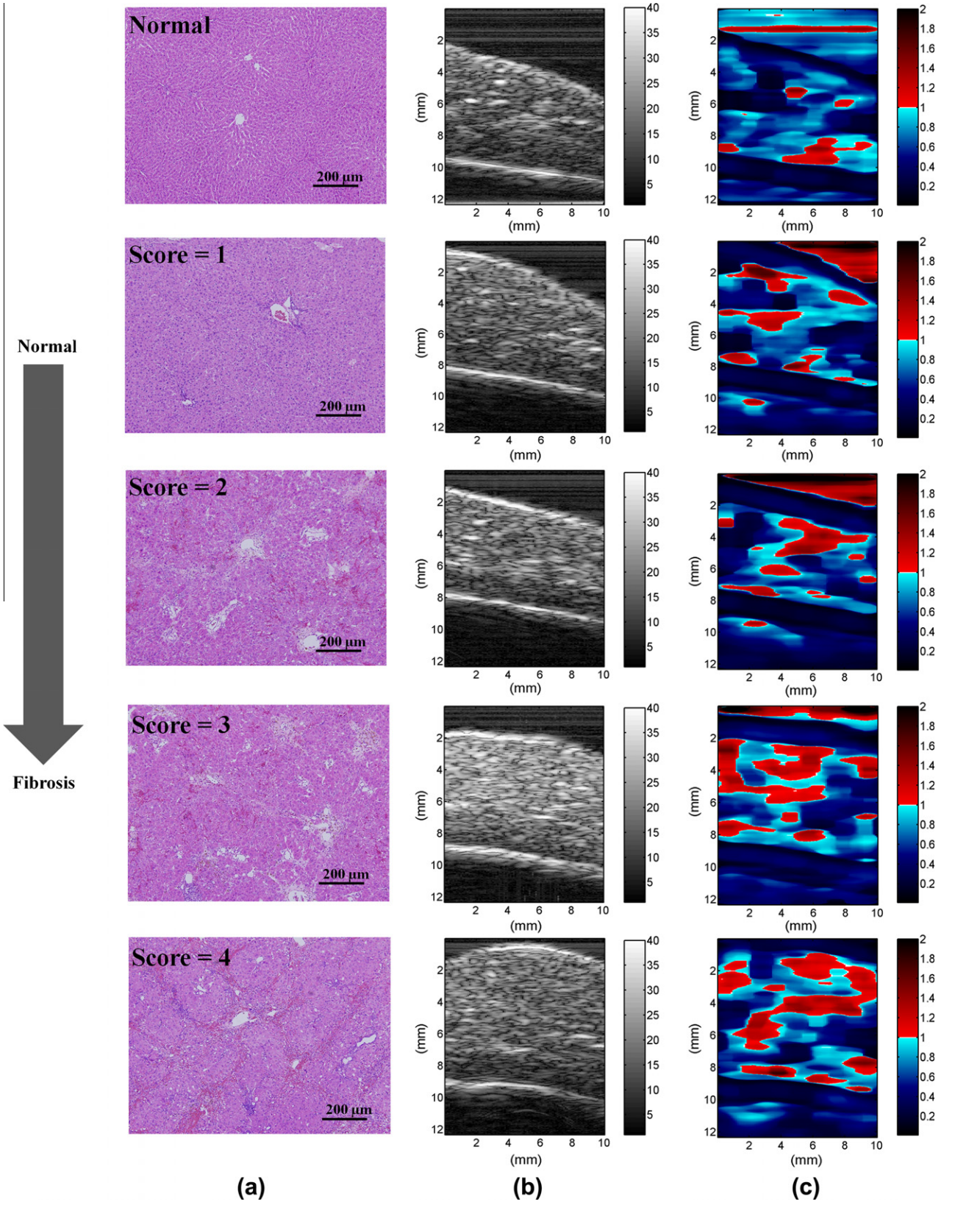

Fig. 3. (a) H&E-stained sections (100 × magnification), (b) B-mode, and (c) Nakagami images of rat livers with different degrees of liver fibrosis.

tings, and algorithm were used to form the Nakagami image. Different features of the Nakagami artifact corresponding to the background may be caused by the effects of white noise and the damping signal that are dependent on the characteristics of the RF cables that are used.

Background white noise not only produces artifacts but also affects the usefulness of the Nakagami image. Owing to white noise typically behaving as a random variable with a Gaussian distribution having a zero mean, the pdf of its envelope will follow Rayleigh statistics. The coupling of background noise with the

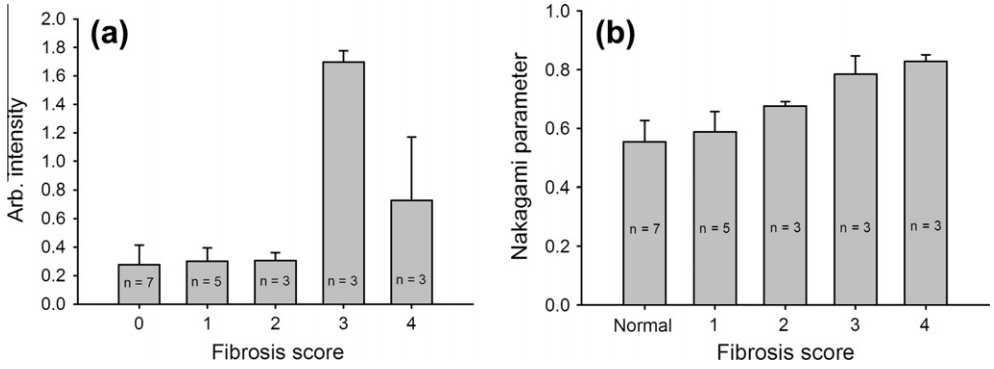

Fig. 4. (a) Image intensity and (b) Nakagami parameter of the rat liver as functions of the fibrosis score.

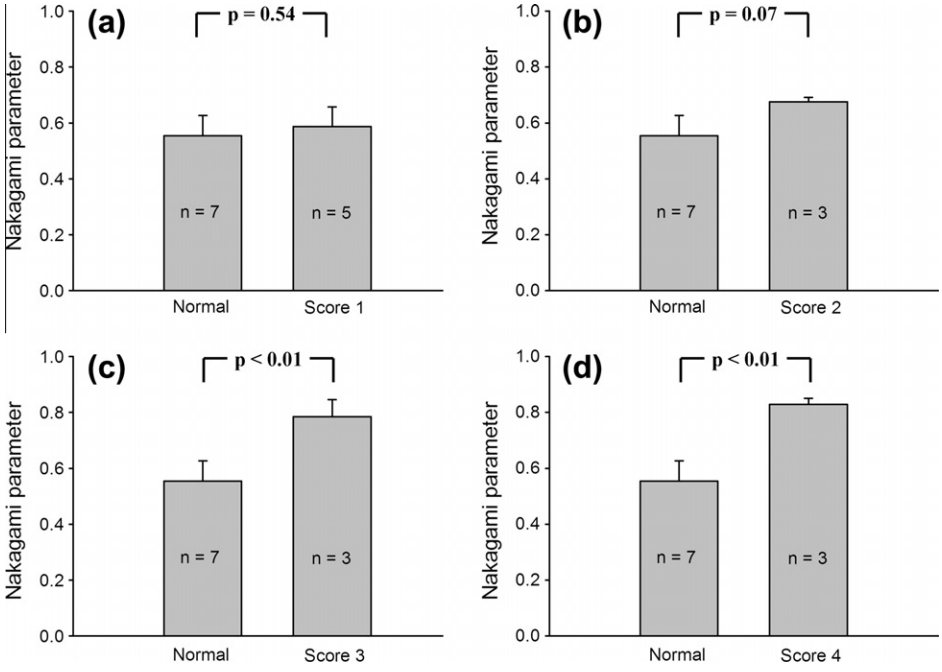

Fig. 5. Comparisons of the Nakagami parameter between normal and fibrotic cases with different Metavir scores.

ultrasound backscattered signals tends to move the total estimated pdf toward a Rayleigh distribution, which in turn moves the Nakagami parameter toward unity [34,35]. A previous study suggested that the signal-to-noise ratio (SNR) of backscattered signals needs to be higher than 11 dB to allow meaningful estimations of the Nakagami parameter when characterizing tissues [34]. For this reason, we roughly evaluated the SNR of the experimental system by calculating the ratio of the echo intensity of the normal liver to that of the background, revealing that the system SNR is approximately 16 dB, which indicates that the current experimental results are reliable. Some techniques of noise reduction and SNR enhancement will be necessary in future *in vivo* applications in order to implement a Nakagami approach with adequate sensitivity and accuracy. For instance, signal processing could be applied to remove some of the noise within the recorded signals. A measurement system with an improved anti-noise ability is also useful in isolating external noises. A highly focused transducer also could enhance the SNR of the backscattered signals [36].

It should be noted that the backscattered signals measured by a focused transducer can be degraded by transducer focusing and beam diffraction, and produce weak and noisy echoes in the far field of the transducer. These factors not only affect the statistical parameter estimation but also limit the datalength acquired for analysis. This previously prompted us to develop the noise-assisted Nakagami parameter based on empirical mode decomposition of noisy backscattered signals to allow scatterer characterization of rat liver tissues using a nonfocused transducer [37]. It has been shown that the noise-assisted Nakagami parameter is useful for assessing liver fibrosis in rats, but it cannot be used for parametric imaging because the wide beam of a nonfocused transducer results in a poor lateral resolution. This explains why the noise-assisted Nakagami parameter is only useful for regional measurements [37].

When visualizing the degree of liver fibrosis in rats, it is better to use the conventional Nakagami parameter estimated with data obtained using a focused transducer. However, the effects of transducer focusing and beam diffraction on the obtained image are unavoidable. Recall that the brightness/depth (B/D) scanning technique can be used to reduce the adverse effects of beam diffraction on the image resolution [38,39]. Future studies should investigate combining B/D scan and image reconstruction techniques in order to further develop multifocus Nakagami imaging for enhancing the usefulness of the Nakagami image in fibrosis assessments.

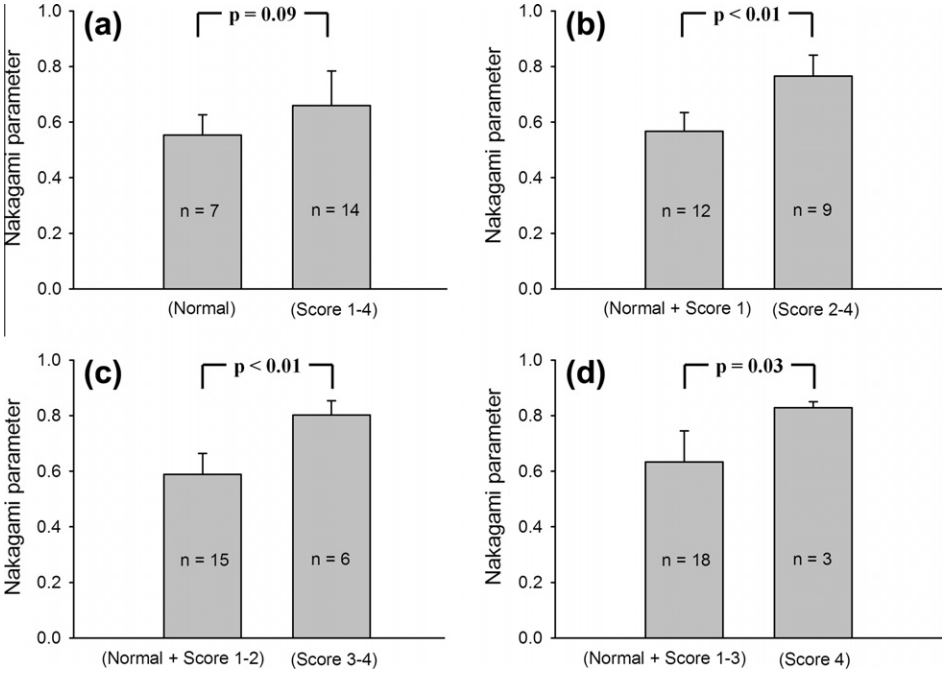

Fig. 6. Comparisons of the Nakagami parameter between group pairs.

In summary, this study performed ultrasound scanning of rat livers *in vitro* to explore the feasibility of using the Nakagami image to assess liver fibrosis in rats. The obtained experimental results demonstrated that the Nakagami image has the ability to visualize the degree of liver fibrosis and to score the liver fibrosis by estimating the Nakagami statistical parameter. The Nakagami image is obtained using a standard pulse-echo system configuration, and therefore it may be combined with the conventional B-scan image, thereby allowing researchers to simultaneously observe the structures and characterize the scatterers within rat livers. The Nakagami image has the potential to serve as a functional imaging tool for animal studies of liver fibrosis.

Acknowledgements

This work was supported in part by the National Science Council of the Republic of China (Taiwan) under Grant No. NSC99-2218-E-182-009 and the Department of Industrial Technology, the Ministry of Economic Affairs of the Republic of China (Taiwan), under Grant No. 99-EC-17-A-19-S1-140.

References

[1] G.M. Lauer, B.D. Walker, Hepatitis C virus infection, N. Engl. J. Med. 345 (2001) 41–52.
[2] A. Regev, M. Berho, L.J. Jeffers, C. Milikowski, E.G. Molina, N.T. Pyrsopoulos, Z.Z. Feng, K.R. Reddy, E.R. Schiff, Sampling error and intraobserver variation in liver biopsy in patients with chronic HCV infection, Am. J. Gastroenterol. 97 (2002) 2614–2618.
[3] P. Bedossa, D. Dargere, V. Paradise, Sampling variability of liver fibrosis in chronic hepatitis C, Hepatology 38 (2003) 1449–1457.
[4] J.P. Iredale, R.C. Benyon, J. Pickering, M. McCullen, M. Northrop, S. Pawley, C. Hovell, M.J. Arthur, Mechanisms of spontaneous resolution of rat liver fibrosis. Hepatic stellate cell apoptosis and reduced hepatic expression of metalloproteinase inhibitors, J. Clin. Invest. 102 (1998) 538–549.
[5] K.L. Yang, K.C. Hung, W.T. Chang, E.I. Li, Establishment of an early liver fibrosis model by the hydrodynamics-based transfer of TGF-beta1 gene, Comp. Hepatol. 19 (2007) 1–9.
[6] T. Fujii, B.C. Fuchs, S. Yamada, G.Y. Lauwers, Y. Kulu, J.M. Goodwin, M. Lanuti, K.K. Tanabe, Mouse model of carbon tetrachloride induced liver fibrosis: Histopathological changes and expression of CD133 and epidermal growth factor, BMC Gastroenterol. 10 (2010) 1–11.
[7] S.K. Venugopal, J. Jiang, T.H. Kim, Y. Li, S.S. Wang, N.J. Torok, J. Wu, M.A. Zern, Liver fibrosis causes downregulation of miRNA-150, and miRNA-194 in hepatic stellate cells and their overexpression causes decreased stellate cell activation, Am. J. Physiol. Gastrointest. Liver Physiol. 298 (2010) G101–G106.
[8] B.B. Gosink, S.K. Lemon, W. Scheible, G.R. Leopold, Accuracy of ultrasonography in diagnosis of hepatocellular disease, Am. J. Roentgenol. 133 (1979) 19–23.
[9] E. Walach, A. Shmulewitz, Y. Itzchak, Z. Heyman, Local tissue attenuation images based on pulsed-echo ultrasound scans, IEEE Trans. Biomed. Eng. 36 (1989) 211–221.
[10] B.I. Raju, M.A. Srinivasan, Statistics of envelope of high-frequency ultrasonic backscatter from human skin in vivo, IEEE Trans. Ultrason. Ferroelectr. Freq. Contr. 49 (2002) 871–882.
[11] P.M. Shankar, A general statistical model for ultrasonic backscattering from tissues, IEEE Trans. Ultrason. Ferroelectr. Freq. Contr. 47 (2000) 727–736.
[12] P.M. Shankar, V.A. Dumane, J.M. Reid, V. Genis, F. Forsberg, C.W. Piccoli, B.B. Goldberg, Classification of ultrasonic B-mode images of breast masses using Nakagami distribution, IEEE Trans. Ultrason. Ferroelectr. Freq. Contr. 48 (2001) 569–580.
[13] M.P. Wachowiak, R. Smolikova, G.D. Tourassi, A.S. Elmaghraby, General ultrasound speckle models in determining scatterer density, P. SPIE 4687 (2002) 285–295.
[14] G. Cloutier, M. Daronatand, D. Savery, D. Garcia, L.G. Durand, F.S. Foster, Non-Gaussian statistics and temporal variations of the ultrasound signal backscattered by blood at frequencies between 10 and 58 MHz, J. Acoust. Soc. Am. 116 (2004) 566–577.
[15] C.C. Huang, S.H. Wang, Statistical variations of ultrasound signals backscattered from flowing blood, Ultrasound Med. Biol. 33 (2007) 1943–1954.
[16] P.M. Shankar, Statistical modeling of scattering from biological media, J. Acoust. Soc. Am. 111 (2002) 2463.
[17] R. Kolář, R. Jirik, J. Jan, Estimator comparison of the Nakagami-m parameter and its application in echocardiography, Radioengineering 13 (2004) 8–12.
[18] F. Davignon, J.F. Deprez, O. Basset, A parametric imaging approach for the segmentation of ultrasound data, Ultrasonics 43 (2005) 789–801.
[19] P.H. Tsui, C.C. Chang, Imaging local scatterer concentrations by the Nakagami statistical model, Ultrasound Med. Biol. 33 (2007) 608–619.
[20] P.H. Tsui, C.K. Yeh, C.C. Chang, W.S. Chen, Performance evaluation of ultrasonic Nakagami image in tissue characterization, Ultrason. Imaging 30 (2008) 78–94.
[21] P.H. Tsui, C.C. Huang, C.C. Chang, S.H. Wang, K.K. Shung, Feasibility study of using high-frequency ultrasonic Nakagami imaging for characterizing the cataract lens in vitro, Phys. Med. Biol. 52 (2007) 6413–6425.
[22] P.H. Tsui, C.C. Huang, L. Sun, S.H. Dailey, K.K. Shung, Characterization of lamina propria and vocal muscle in human vocal fold tissue by ultrasound Nakagami imaging, Med. Phys. 38 (2011) 2019–2026.
[23] P.H. Tsui, C.K. Yeh, C.C. Chang, Y.Y. Liao, Classification of breast masses by ultrasonic Nakagami imaging, Phys. Med. Biol. 53 (2008) 6027–6044.
[24] P.H. Tsui, Y.Y. Liao, C.C. Chang, W.H. Kuo, K.J. Chang, C.K. Yeh, Classification of benign and malignant breast tumors by 2-D analysis based on contour

description and scatterer characterization, IEEE Trans. Med. Imaging 29 (2010) 513–522.
[25] P.H. Tsui, Y.L. Wan, C.C. Huang, M.C. Wang, Effect of adaptive threshold filtering on ultrasonic Nakagami parameter to detect variation in scatterer concentration, Ultrason. Imaging 32 (2010) 229–242.
[26] Y.Y. Liao, P.H. Tsui, C.K. Yeh, Classification of benign and malignant breast tumors by ultrasound B-scan and Nakagami-based images, J. Med. Biol. Eng. 30 (2010) 307–312.
[27] J. George, K.R. Rao, R. Stenr, G. Chandrakasan, Dimethylnitrosamine-induced liver injury in rats: the early deposition of collagen, Toxicology 156 (2001) 129–138.
[28] Z.F. Lu, J.A. Zagzebski, F.T. Lee, Ultrasound backscatter and attenuation in human liver with diffuse disease, Ultrasound Med. Biol. 25 (1999) 1047–1054.
[29] M. Meziri, W.C.A. Pereirab, A. Abdelwahabc, C. Degottd, P. Laugierc, In vitro chronic hepatic disease characterization with a multiparametric ultrasonic approach, Ultrasonics 43 (2005) 305–313.
[30] A. Guimond, M. Teletin, E. Garo, A. D'Sa, M. Selloum, M.F. Champy, J.L. Vonesch, L. Monassier, Quantitative ultrasonic tissue characterization as a new tool for continuous monitoring of chronic liver remodelling in mice, Liver Int. 27 (2007) 854–864.
[31] R. Bataller, D.A. Brenner, Liver fibrosis, J. Clin. Invest. 115 (2005) 209–218.
[32] H. Yamada, M. Ebara, T. Yamaguchi, S. Okabe, H. Fukuda, M. Yoshikawa, T. Kishimoto, H. Matsubara, H. Hachiya, H. Ishikura, H. Saisho, A pilot approach for quantitative assessment of liver fibrosis using ultrasound: preliminary results in 79 cases, J. Hepatol. 44 (2006) 68–75.
[33] T. Yamaguchi, H. Hachiya, Proposal of a parametric imaging method for quantitative diagnosis of liver fibrosis, J. Med. Ultrason. 37 (2010) 155–166.
[34] P.H. Tsui, S.H. Wang, C.C. Huang, C.Y. Chiu, Quantitative analysis of noise influence on the detection of scatterer concentration by Nakagami parameter, J. Med. Biol. Eng. 25 (2005) 45–51.
[35] P.H. Tsui, C.K. Yeh, C.C. Chang, Noise effect on the performance of Nakagami image in ultrasound tissue characterization, J. Med. Biol. Eng. 28 (2008) 197–202.
[36] S.H. Wang, K.K. Shung, An approach for measuring ultrasonic backscattering from biological tissues with focused transducers, IEEE Trans. Biomed. Eng. 44 (1997) 549–554.
[37] P.H. Tsui, C.C. Chang, M.C. Ho, Y.H. Lee, Y.S. Chen, C.C. Chang, N.E. Huang, Z.H. Wu, K.J. Chang, Use of nakagami statistics and empirical mode decomposition for ultrasound tissue characterization by a nonfocused transducer, Ultrasound Med. Biol. 35 (2009) 2055–2068.
[38] C. Passmann, H. Ermert, T. Auer, K. Kaspar, S. el-Gammal, P. Altmeyer, In vivo ultrasound biomicroscopy, IEEE Ultrason. Symp. 2 (1993) 1015–1018.
[39] C.K. Yeh, C.H. Chunh, C.C. Chuang, A Novel Multi-Focus Image Reconstruction Technique in High Frequency Ultrasound, IEEE Ultrason. Symp. 1 (2006) 2218–2221.